

# Journal of Materials Chemistry A

Accepted Manuscript



This is an *Accepted Manuscript*, which has been through the Royal Society of Chemistry peer review process and has been accepted for publication.

*Accepted Manuscripts* are published online shortly after acceptance, before technical editing, formatting and proof reading. Using this free service, authors can make their results available to the community, in citable form, before we publish the edited article. We will replace this *Accepted Manuscript* with the edited and formatted *Advance Article* as soon as it is available.

You can find more information about *Accepted Manuscripts* in the [Information for Authors](#).

Please note that technical editing may introduce minor changes to the text and/or graphics, which may alter content. The journal's standard [Terms & Conditions](#) and the [Ethical guidelines](#) still apply. In no event shall the Royal Society of Chemistry be held responsible for any errors or omissions in this *Accepted Manuscript* or any consequences arising from the use of any information it contains.

# Porous trimetallic Au@Pd@Ru nanoparticle system: Synthesis, characterisation and efficient dye degradation and removal

Cite this: DOI: 10.1039/x0xx00000x

Received 00th January 2012,  
Accepted 00th January 2012

DOI: 10.1039/x0xx00000x

www.rsc.org/

Anupam Sahoo, Suman Kumar Tripathy, Niranjana Dehury, and Srikanta Patra\*

A facile room temperature one-pot synthesis of trimetallic porous Au@Pd@Ru nanoparticles (Au@Pd@RuNPs) has been developed. The trimetallic nanoparticles have been prepared by the successive sacrificial oxidation of cobalt nanoparticles (CoNPs). The average particle size for Au@Pd@RuNPs is 110 nm. The porous nature and the presence of Au, Pd and Ru have been confirmed via TEM, FE-SEM and EDS analyses. The trimetallic nanoparticles have shown excellent catalytic activity towards the reduction of *p*-nitrophenol and efficient degradation of various azo dyes. This has further been extended towards the removal of colour from the waste water via the catalytic degradation of azo dyes. Moreover, the produced amine can be eliminated from the waste water via its sorption on an industrial solid waste dolochar.

## Introduction

The development of multimetallic core-shell or alloy nanoparticles has gained a significant attention in recent decades both from the fundamental as well as application perspectives.<sup>1-11</sup> This is primarily because of the fact that multimetallic nanoparticles often provide unique optoelectronic, electrochemical, chemical and catalytic properties which are significantly different from their monometallic counterparts.<sup>1, 12-19</sup> Addition of a second metal onto the existing metal enhances its properties like activity, stability and selectivity by ensemble or ligand effect.<sup>1, 17, 18, 20, 21</sup> The properties of multimetallic nanoparticles can also be manipulated by varying the chemical composition.<sup>14-16, 22-27</sup> The activity of nanoparticles can further be enhanced by making porous structures.<sup>16, 27-29</sup> Continuing efforts are being in place towards the development of such materials in order to achieve the desired properties and activities. In this context, several bimetallic core-shell type nanomaterials of both solid and porous structures have been developed and extensively studied.<sup>11-13, 15-19, 26, 30-32</sup> In contrast, heterotrimetallic nanoparticles are relatively less common, although they can show interesting properties as compared to their monometallic and bimetallic counterparts.<sup>3, 19, 21, 33-36</sup> Moreover, the trimetallic porous structured nanoparticles are yet to be explored. Au, Pd and Ru are well known for their excellent catalytic and electrocatalytic properties. The catalytic and electrocatalytic features of bimetallic nanoparticles derived from Au-Pd,<sup>15, 32, 37-42</sup> Au-Ru<sup>32, 43-49</sup> or Pd-Ru<sup>50-52</sup> have been extensively studied. However, heterotrimetallic nanoparticle consisting of Au, Pd and Ru in solid or porous form has not yet been explored. Thus, the present article intends to highlight the development of trimetallic porous structured Au@Pd@Ru nanoparticles (Au@Pd@RuNPs) and to study their reactivity towards

catalytic *p*-nitrophenol (PNP) reduction and azo dye degradation.

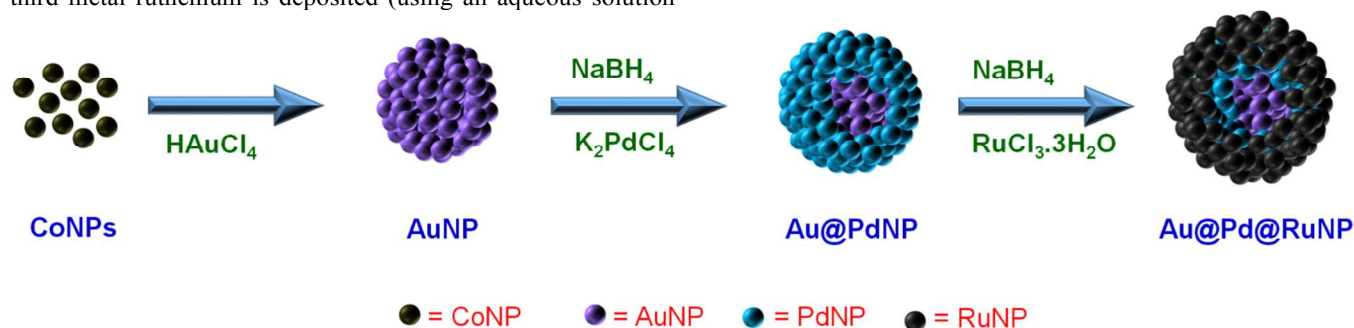
Herein, we describe a facile room-temperature synthesis of trimetallic porous Au@Pd@RuNPs via stepwise spontaneous oxidation of cobalt nanoparticles (CoNPs). The porous structure of the synthesised core-shell nanoparticles has been confirmed by FE-SEM and TEM analysis. In addition, the synthesised nanoparticles have been subjected to test the catalytic activity towards the reduction of PNP and various azo compounds. Further, the activity of the Au@Pd@RuNPs is extended to decolorise the coloured waste water (synthetic and industrial) via catalytic decomposition of the azo bond and possible remediation from the produced toxic amine by the efficient sorption using dolochar (an industrial solid waste) to purify waste water.

## Results and discussion

The trimetallic porous Au@Pd@RuNPs have been prepared by the stepwise galvanic displacement of CoNPs (Scheme 1) (See Experimental Section). The CoNPs have been prepared by the reduction of aqueous CoCl<sub>2</sub> solution by a strong reducing agent NaBH<sub>4</sub>.<sup>27, 28</sup> Citrate is acting as capping agent to stabilise the formed CoNPs. Addition of as synthesised CoNPs solution to the aqueous solution of HAuCl<sub>4</sub> leads to the spontaneous reduction of Au<sup>3+</sup> ions to Au<sup>0</sup> by the sacrificial oxidation of Co<sup>0</sup>/Co<sup>2+</sup> ( $E_{\text{Au}^{3+}/\text{Au}^0} + 0.994 \text{ V}$  and  $E_{\text{Co}^{2+}/\text{Co}^0} - 0.277 \text{ V}$  versus SHE). The dark blackish brown colour of the solution has changed to violet indicating the formation of porous Au nanoparticles (AuNPs). A 0.1% polyvinylpyrrolidone (PVP) has been added to the solution for better stabilisation. After allowing sufficient time, the oxidised Co<sup>2+</sup> ions in solution have further been reduced by NaBH<sub>4</sub> and core-shell type Au@CoNPs are obtained. Palladium has been spontaneously

deposited onto the porous AuNPs by the sacrificial oxidation of Co layer of Au@CoNPs using an aqueous solution of  $K_2[PdCl_4]$  ( $E_{Pd^{2+}/Pd^0} + 0.915$  V versus SHE). Subsequently, a third metal ruthenium is deposited (using an aqueous solution

of  $RuCl_3 \cdot 3H_2O$  ( $E_{Ru^{3+}/Ru^0} + 0.68$  V versus SHE)) by repeating the similar procedure and trimetallic porous Au@Pd@RuNPs are obtained (Scheme 1).



**Scheme 1.** Schematic representation for the preparation of porous AuNPs, Porous, Au@PdNPs and porous Au@Pd@RuNPs.

Formation of porous AuNPs, porous Au@PdNPs and porous Au@Pd@RuNPs are realised by the distinct colour change using UV-Vis spectroscopy. Figure 1 represents the UV-Vis spectra of the nanoparticles in solution. The spontaneous reduction of  $Au^{3+} \rightarrow Au^0$  by  $Co^0$  is witnessed by the generation of a surface plasmon resonance (SPR) band at 667 nm indicating the formation of porous Au nanospheres. The disappearance of characteristic SPR band of porous AuNPs upon addition of second or third metals Pd or Ru by sacrificial oxidation of  $Co^0$  indicating the deposition of Pd or Ru onto the Au surface (Fig. 1).

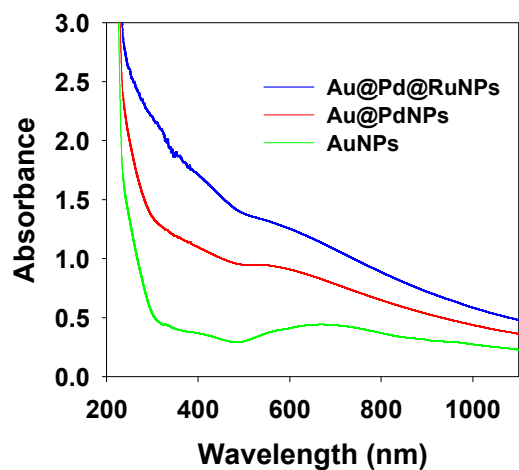


**Fig. 1** UV-Vis spectra of porous AuNPs, porous Au@PdNPs and porous Au@Pd@RuNPs in water.

The porous nature of the nanoparticles have been confirmed by the FE-SEM and TEM analysis (Fig. 2 and S1). The FE-SEM images of all the nanoparticles have shown blackberry like structure. The bimetallic Au@PdNPs and trimetallic Au@Pd@RuNPs are formed via the deposition of smaller sized PdNPs and RuNPs, onto the surface of AuNPs and Au@PdNPs, respectively (Fig. 2a and S1a and b). The FE-SEM images have further revealed that the formed AuNPs, Au@PdNPs and Au@Pd@RuNPs are moderately monodispersed and the average size of the nanoparticles are 90 nm, 105 nm and 110 nm, respectively (Fig. 2, S1 and S2). Further, the TEM image of AuNPs, Au@PdNPs and Au@Pd@RuNPs have also revealed porous structures with moderately good monodispersity (Fig. 2b and S1). The EDS analysis of the

selected region of nanoparticles indicate the presence of Au, Pd and Ru metals in AuNPs, Au@PdNPs and Au@Pd@RuNPs (Fig. 2c, and S1e and f).

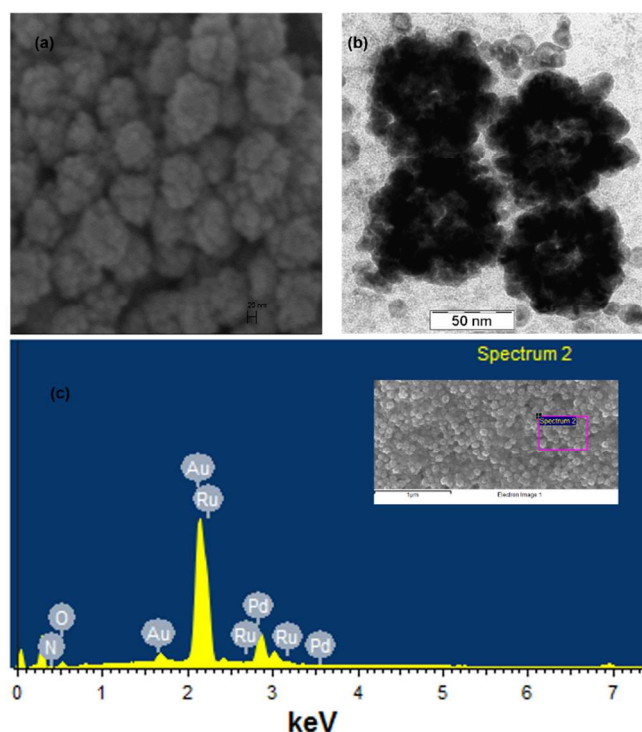


**Fig. 2** (a) FE-SEM and (b) TEM images, and (c) EDS spectra of Au@Pd@RuNPs. Inset of (c) represents the region selected for recording the EDS spectra.

The AuNPs, PdNPs, RuNPs and their bimetallic analogues are well known for their catalytic and electrocatalytic activities.<sup>53-63</sup> To test the catalytic activity of the synthesised nanoparticles, standard *p*-nitrophenol (PNP) reduction by  $NaBH_4$  have been conducted. The disappearance of the distinct band at 400 nm during the reduction of PNP in presence of the catalysts has been monitored by UV-Vis spectroscopy (Fig. 3a). It is well documented that this reaction can be catalysed by noble metals.<sup>16, 53-56</sup> To understand the variation of reactivity of the nanoparticles (porous AuNPs, porous Au@PdNPs and porous Au@Pd@RuNPs) kinetic measurements of reduction of 0.1

mM PNP in the presence of 10 mM NaBH<sub>4</sub> and a fixed amount of synthesised nanoparticles has been studied (Fig. 3). It is observed that all the synthesised nanoparticles catalysed the reduction of PNP efficiently, however, the rate of the reaction significantly varies between the nanoparticles (Fig. 3b). The trimetallic Au@Pd@RuNPs has shown better reactivity than the corresponding bimetallic Au@PdNPs and monometallic AuNPs (porous Au@Pd@RuNPs > porous Au@PdNPs > porous AuNPs) indicating the importance of second or third metal into the nanoparticle system. The observed rate of reaction is pseudo-first order with respect to PNP. The calculated rate constants are varying significantly for different nanoparticles (Table 1). Interestingly, the trimetallic Au@Pd@RuNPs has been able to complete at least six more catalytic cycle with comparable efficiency during the repeated addition of PNP into the same reaction vessel after the completion of first catalytic cycle. This observation signifies high efficiency and repeatability of the present catalytic system for the decomposition of PNP.

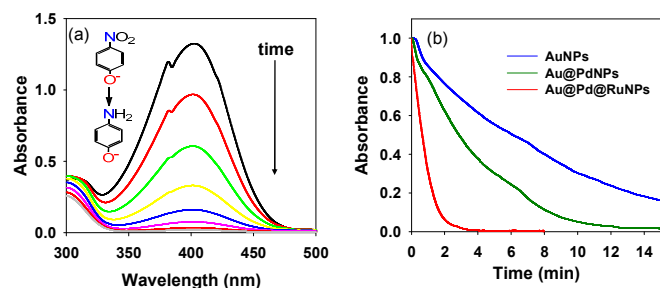


**Fig. 3** (a) UV-Vis spectra of the catalytic reduction of PNP in presence of Au@Pd@RuNPs and (b) normalised time dependent catalytic reduction of PNP at 400 nm in presence of Au@Pd@RuNPs, Au@PdNPs and AuNPs in tris buffer (pH 9.0). [PNP] = 0.1 mM; [NPs] = 0.5 pM; [NaBH<sub>4</sub>] = 10 mM.

**Table 1** Summary of the observed rate constants toward the reduction of PNP and degradation of various dyes in the presence of nanocatalysts in tris buffer solution (pH 9.0). [PNP] = 0.1 mM, [NaBH<sub>4</sub>] = 10 mM, [NP] = 0.5 pM; [dye] = 0.1 mM.

Nanoparticles	Rate constant (s <sup>-1</sup> )			
	PNP	CR	RR-120	RB-05
AuNPs	1.99 ± 0.04 x 10 <sup>-3</sup>	1.74 ± 0.49 x 10 <sup>-4</sup>	-----	-----
Au@PdNPs	5.09 ± 0.34 x 10 <sup>-3</sup>	7.20 ± 0.12 x 10 <sup>-4</sup>	-----	-----
Au@Pd@RuNPs	2.42 ± 0.12 x 10 <sup>-2</sup>	2.49 ± 0.65 x 10 <sup>-2</sup>	1.34 ± 0.29 x 10 <sup>-2</sup>	9.49 ± 0.74 x 10 <sup>-2</sup>

We next extend the catalytic activity of the nanoparticles towards the degradation of azo compounds. It is well known that the effluents containing azo dyes cause severe problem to aquatic life. The dyes discharged as industrial waste from the textile or other related industries not only cause water pollution but also pose a health risk to human.<sup>64</sup> The dyes are very stable and are not degraded easily. Thus, facile catalytic degradation of dyes could be a viable option to get rid of the dye based pollution. Reductive cleavage of azo dyes could eliminate the colour from the solution. It is well documented that the degradation of azo (-N=N-) bond can be efficiently done by various metal nanoparticles.<sup>65-75</sup> Thus, to test the reactivity of our synthesised nanocatalysts towards the degradation of azo dyes congo red (CR) has been taken as reference. The kinetics of CR dye degradation (disappearance of the band at 498 nm)

has been monitored by UV-Vis spectroscopy (Fig. 4). The degradation of CR is monitored both in neutral (pH 7.0) as well as in tris buffer (pH 9.0) solution. In both cases the degradation of CR in presence of trimetallic Au@Pd@RuNPs nanocatalyst has been completed in approximately 4 minutes and the rate of degradation of CR are almost the same. Considering the controlled decomposition of NaBH<sub>4</sub> in alkaline medium, pH 9.0 has been selected for further studies. The corresponding bimetallic Au@PdNPs and monometallic AuNPs have shown much inferior reactivity than the trimetallic nanoparticles (Fig. 4b and Table 1) indicating the importance of second or third metals into the catalyst system. The kinetic analysis of the degradation of CR in presence of Au@Pd@RuNPs (linear dependence of ln(A<sub>0</sub>/A<sub>t</sub>) vs time) suggests first order reaction with respect to the dye.

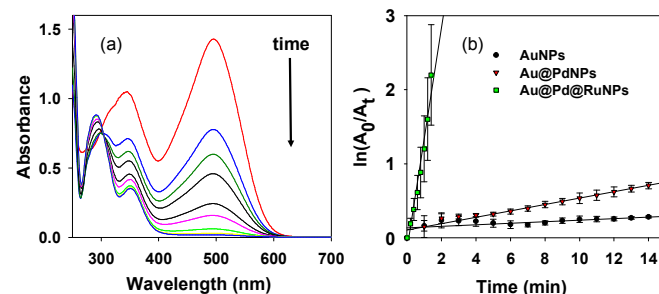


**Fig. 4** (a) UV-Vis spectra of the catalytic reduction of CR in presence of Au@Pd@RuNPs and (b) time dependent catalytic degradation of CR at 498 nm in presence of Au@Pd@RuNPs, Au@PdNPs and AuNPs in tris buffer (pH 9.0). [CR] = 0.1 mM; [NPs] = 0.5 pM; [NaBH<sub>4</sub>] = 10 mM.

To test the generality of the dye degradation, the other dyes such as reactive red (RR-120) and reactive black (RB-5) have been used (Scheme S1). Figure 5 represents the degradation of various azo dyes at pH 9.0 using specific concentration of nanocatalyst. It is observed that all the dyes are efficiently degraded (~ 4 minutes) in the presence of trimetallic nanocatalyst Au@Pd@RuNPs (Fig. 5). The rate of degradation of the dyes follow the order: RB-5 > CR > RR-120. The results suggest that the trimetallic Au@Pd@RuNPs nanocatalyst system could be useful for the degradation of various azo based dyes. Notably, the same Au@Pd@RuNPs trimetallic nanocatalyst is able to repeat the catalytic cycles at least six times with comparable efficiency for all the three dyes.

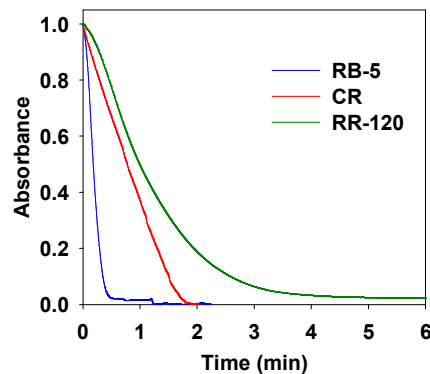


**Fig. 5** Normalised time dependent catalytic degradation of CR at 498 nm, RR-120 at 535 nm and RB-5 at 595 nm in presence of Au@Pd@RuNPs nanocatalyst in tris buffer (pH 9.0). [dye] = 0.1 mM; [NPs] = 0.5 pM; [NaBH<sub>4</sub>] = 10 mM.

We next study the removal of produced aromatic amines from the reaction mixture (Scheme S1). The aromatic amines are also well-known carcinogenic agents which cause severe problems in both aquatic as well as human life.<sup>76-78</sup> In general, enzymatic reduction (using the enzymes tyrosinase, oxido-reductase, laccases, etc.) or aerobic/anaerobic biodegradation (using different types of micro-organism) of amines are commonly used for the removal of aromatic amines.<sup>73, 79-89</sup> Nevertheless, the methods are tedious, cost inefficient and need special precaution towards culturing microbial media and maintaining the activity of enzymes.<sup>90-92</sup> To overcome these limitations we have taken a simple and milder strategy for the removal of amines via their sorption onto a porous substrate. Dolochar is a carbonaceous solid waste obtained from sponge iron industry. It is having requisite porosity and large surface area.<sup>93</sup> Dolochar has thus been used for the efficient removal of various ions such as  $\text{Cd}^{2+}$ ,  $\text{Cr}^{6+}$ ,  $\text{PO}_4^{3-}$ , etc.<sup>93, 94</sup> It is therefore assumed that dolochar can also sorb amines efficiently. To test the sorption of amine on dolochar various aromatic amines such as benzidine, 2-aminophenol, 4-aminophenol and 3, 4-dimethoxyaniline have been used (Fig. 6). The UV-Vis spectra of the amines showing the bands around 300 nm and 250 nm (Fig. 6 (i)) have diminished significantly after the treatment of dolochar (Fig. 6 (ii)) suggesting their sorption into porous dolochar.

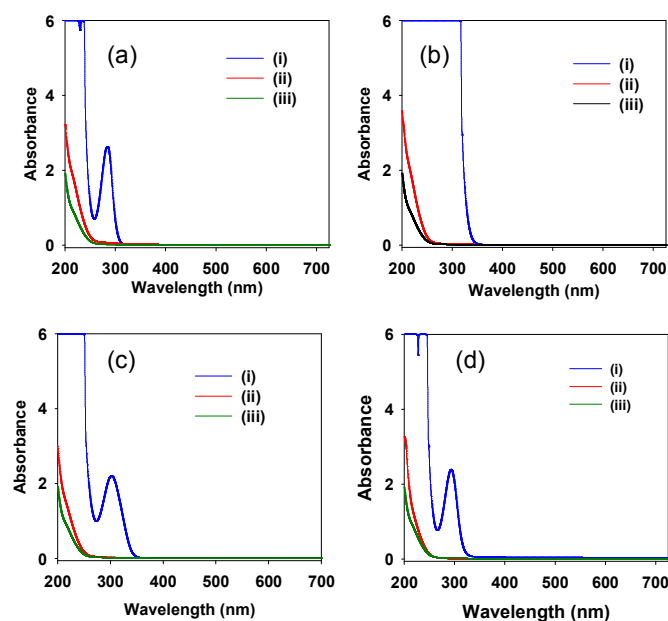


**Fig. 6** UV-Vis spectra of 1.0 mM ( $10 \text{ cm}^3$ ) solution of (a) 2-aminophenol, (b) benzidine, (c) 4-aminophenol and (d) 3,4-dimethoxyaniline before (i) and after (ii) their sorption on 1000 mg dolochar for 12 h and (iii) blank in tris buffer (pH 9.0).

We next extend this strategy to sorb produced amines during the catalytic degradation of CR and other dyes. It is observed that during the degradation of CR new bands around 250 nm and 300 nm have developed (Fig. 4a) which is due to the formation of corresponding amines (Scheme S1).<sup>95</sup> Dolochar has been added into the reaction mixture after the degradation of the dye and stirred overnight. The UV-Vis spectra of the solution have shown the bands corresponding to aromatic amines ( $\sim 250 \text{ nm}$  and  $\sim 300 \text{ nm}$ ) have disappeared suggesting the significant sorption of amines (Fig. S3a). Further, the EDS analysis of the treated dolochar also has shown peaks related to

nitrogen indicating the sorption of amines (Fig. S4d). The sorption behaviour of amines from other decomposed dyes (RR-120 and RB-5) have also been tested and similar sorption behaviour is observed ((Fig. S3b and c).

Next, we have extended this to study for the treatment of synthetic waste water. The trimetallic nanocatalyst  $\text{Au@Pd@RuNPs}$  has shown efficient dye degradation followed by removal of in situ generated amines from the solution by using dolochar (Fig. 7a). This encouraging result has prompted us to examine the decolourisation of real industrial waste water (See Experimental Section) using  $\text{Au@Pd@RuNPs}$  nanocatalyst followed by the sorption of produced amines in dolochar. It is observed that the synthesised nanocatalyst efficiently decolorise coloured waste water and remove corresponding amines (Fig. 7b). The present one-pot method for the degradation of azo dyes is much simpler and removal of produced amines do not require any tedious biological methods. Moreover, the present method generates solid waste from aqueous solution by using another waste dolochar. Handling solid waste is much convenient than handling the liquid waste. Thus, the present report would be very useful for the efficient removal of colour and corresponding amines from the textile based waste water.

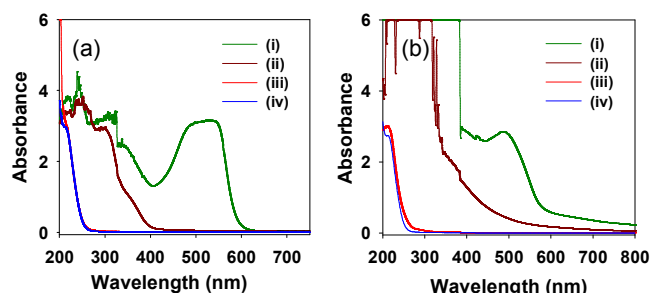


**Fig. 7** Absorption spectra of (a) synthetic waste water and (b) industrial waste water (i) before and (ii) after the reduction by  $\text{NaBH}_4$  in presence of  $\text{Au@Pd@RuNPs}$  and (iii) after the treatment of dolochar for 12 h and (iv) blank.  $[\text{NPs}] = 0.5 \text{ pM}$ ;  $[\text{NaBH}_4] = 50 \text{ mM}$  and dolochar = 750 mg for (a) and 1500 mg for (b). The volume of synthetic and industrial waste water taken for this experiment was  $10 \text{ cm}^3$ .

## Conclusions

In conclusion, we have developed a facile room temperature method for the preparation of trimetallic porous  $\text{Au@Pd@RuNPs}$  nanocatalyst system via the successive sacrificial oxidation of CoNPs. The porous nature and elemental composition of the nanocatalyst has been confirmed by TEM and FE-SEM studies, and EDS analysis. The nanocatalyst has shown excellent catalytic reactivity towards the reduction of PNP and degradation of azo based dyes. Further the toxic amines produced during degradation of azo dyes have been removed via the sorption on solid industrial waste dolochar. The nanocatalyst has shown efficient removal of colours and in situ generated toxic amines from industrial waste water are eliminated by simple sorption on a porous solid waste (dolochar) which is much more convenient than the traditional biological processes. Further, the present report demonstrate the generation of solid waste from waste water which is convenient for waste management. This is the first example of the trimetallic porous  $\text{Au@Pd@RuNPs}$  system which is important both from the synthetic and catalytic point

of view. Moreover, we believe that the present report would be an important addition towards the nanocatalyst based efficient removal of azo-based dyes and treatment of textile waste water.

## Experimental

### Materials

All chemicals were purchased from commercial sources and used as received. All glasswares were cleaned with aqua-regia and thoroughly rinsed with copious amount of doubly distilled water. All aqueous solutions and buffers were prepared by doubly distilled water. All the inert atmospheric reactions were conducted under dinitrogen atmosphere using standard Schlenk technique. Nitrogen gas was purged throughout during the preparation of nanoparticles. All the reactions were carried out at 25 °C unless specified. The molar concentration of nanoparticles in solution was calculated by following the previously reported procedure and is found to be ~ 5.0 pM.<sup>16, 96, 97</sup> The solid waste dolochar was collected from the Orissa Pollution Control Board and processed by following reported procedure.<sup>94</sup> The synthetic waste water was prepared as per the reported procedure.<sup>94, 98</sup> The industrial waste water was collected from the local textile industry at Khordha Industrial Area, Khordha, Orissa, India.

### Instrumentation

UV-Vis spectra were obtained by using a Perkin Elmer Lambda 35 spectrophotometer. The Dynamica Velocity 18R refrigerated centrifuge instrument was used for the separation of nanoparticles. FE-SEM images and EDS analysis were carried out using Zeiss Merlin compact Microscope and Oxford instruments, respectively. TEM analysis were conducted using a JEOL 2000 FX-II Transmission Electron Microscope.

### Synthesis of trimetallic nanoparticles

#### Preparation of porous gold nanoparticles (AuNPs)

Co nanoparticle was prepared by adding 0.1 cm<sup>3</sup> of 0.4 M CoCl<sub>2</sub> solution into 100 cm<sup>3</sup> deaerated aqueous solution containing 8 mM NaBH<sub>4</sub> and 1.0 mM sodium citrate. During the course of reaction, the purple coloured solution was turned to brownish black indicating the formation of CoNPs. Stirring was continued till the evolution of H<sub>2</sub> gas ceased. Nitrogen was purged to the solution throughout the reaction to avoid the oxidation of the formed CoNPs. In parallel, 60 cm<sup>3</sup> of 0.44 mM aqueous HAuCl<sub>4</sub> was deaerated during this time. When the H<sub>2</sub> gas evolution ceased, the HAuCl<sub>4</sub> solution was transferred to CoNPs solution via cannula. As soon as the solution was added, the colour of the solution was changed to deep blue and then violet indicating formation of porous AuNPs. A required amount of PVP (final concentration 0.1 %) was added and the solution was stirred for 2 h at 50 °C. The AuNPs solution was marked as **solution A**. A part of **solution A** was centrifuged at 4 °C at 12000 rpm for 15 minutes to remove the oxidised cobalt. The supernatant was decanted and resuspended in 0.1% PVP. This process was repeated thrice to obtain pure porous AuNPs. This porous AuNPs solution was used for further characterisation and to study the catalytic activity.

#### Preparation of porous Au@Pd nanoparticles (Au@PdNPs)

To a 25 cm<sup>3</sup> deaerated **solution A**, 0.4 cm<sup>3</sup> of 0.5 M NaBH<sub>4</sub> solution was added. Immediately, the blue coloured solution turned to brownish black indicating the deposition of CoNPs layer onto the AuNPs. The solution was then allowed stir at room temperature until the evolution of hydrogen gas ceased. An aqueous solution of 0.31 cm<sup>3</sup> (20 mM) K<sub>2</sub>[PdCl<sub>4</sub>] was added

to the reaction mixture and stirred for 6 h at room temperature and additional 2 h at 50 °C. This black coloured solution was marked as **solution B**. The pure PVP stabilised Au@PdNPs was obtained by following the similar procedure as described for porous AuNPs.

#### Preparation of porous Au@Pd@Ru nanoparticles (Au@Pd@RuNPs)

Similar synthesis procedure was adopted for the preparation of porous Au@Pd@RuNPs from **solution B** as mentioned for the preparation of Au@PdNPs. An aqueous solution of 0.166 mM (final concentration) RuCl<sub>3</sub>·3H<sub>2</sub>O was used for the preparation of Au@Pd@RuNPs.

#### Reduction of *p*-nitrophenol (PNP)

The reduction of *p*-nitrophenol (PNP) using synthesised nanoparticles was monitored by following the procedure reported by Pradhan et al.<sup>56</sup> Briefly, in a standard 1.0 cm<sup>3</sup> quartz cuvette (with 1 cm path length) nanocatalyst (100 μL, 5.0 pM), excess NaBH<sub>4</sub> (100 μL, 100 mM) and 700 μL tris buffer (pH 9.0) were taken and the solution was kept at 25° C for 5 minutes. A 100 μL (1 mM) solution of PNP was added to the reaction mixture and the reduction of PNP was monitored by recording the time-course spectra at 400 nm.

#### Degradation of azo dyes

Nanocatalyst (100 μL, 5.0 pM) and excess NaBH<sub>4</sub> (100 μL, 100 mM) were taken in 700 μL tris buffer (pH 9.0) solution in a standard 1.0 cm<sup>3</sup> quartz cuvette having 1 cm path length and kept for 5 minutes at 25 °C. A 100 μL (1 mM) solution of CR was then added and the time course spectra of the decomposition of CR were recorded at 498 nm. The time course spectra for RB-5 (595 nm) and RR-120 (535 nm) dye were also recorded by following the similar procedure as CR.

#### Sorption of aromatic amines on dolochar

To a 10 cm<sup>3</sup> tris buffer (pH 9.0) solution of 1 mM aromatic amine (2-aminophenol) 1000 mg dolochar was added. The solution was then stirred for 12 h at room temperature. The solution was allowed to settle, filtered and UV-Vis spectrum was recorded. Similar procedure was followed for other aromatic amines (benzidine, 4-aminophenol and 3, 4 dimethoxyaniline).

#### Adsorption of generated aromatic amines on dolochar

The sorption of reduced products (aromatic amines) of congo red dye onto dolochar was carried out by taking 10 cm<sup>3</sup>, 700 mg/dm<sup>3</sup> CR. Before treatment with dolochar the solution was reduced by trimetallic porous Au@Pd@Ru nanocatalyst (100 μL, 5.0 pM) and 100 mM NaBH<sub>4</sub>. After complete decolourisation and decomposition of NaBH<sub>4</sub> (12 h), dolochar (400 mg) was added to the reaction mixture. The mixture was stirred overnight at 250 rpm at room temperature. The sorption of the produced amines were monitored using UV-Vis spectroscopy by observing the decrease in the band intensities of corresponding amines. Similar procedure was adopted for 10 cm<sup>3</sup>, 700 mg/dm<sup>3</sup> RR-120 and 1000 mg/dm<sup>3</sup> RB-5.

#### Preparation of synthetic waste water

Synthetic waste water was prepared by mixing starch (1000 mg/dm<sup>3</sup>), sucrose (600 mg/dm<sup>3</sup>), CR(100 mg/dm<sup>3</sup>), RR-120(100 mg/dm<sup>3</sup>), acetic acid (200 mg/dm<sup>3</sup>), sulphuric acid (300 mg/dm<sup>3</sup>), sodium hydroxide (500 mg/dm<sup>3</sup>), sodium carbonate (500 mg/dm<sup>3</sup>), sodium chloride (3000 mg/dm<sup>3</sup>),

Sodium dodecyl sulphate (100 mg/dm<sup>3</sup>) in 1000 cm<sup>3</sup> volumetric flask. The pH of the resulting solution was 9.5.

### Treatment of synthetic and Industrial waste water with dolochar

10 cm<sup>3</sup> of synthetic waste water was decolourised by adding 100 μL, 5.0 pM Au@Pd@RuNPs and 50 mM NaBH<sub>4</sub>. After decolourisation, the solution was treated with 750 mg dolochar. The solution was then stirred for 12 h at room temperature. UV-Vis spectra of the solution was recorded after filtration. Similar procedure was adopted for the treatment of industrial waste water. The amount of dolochar was taken 1500 mg for the sorption of produced amines from industrial waste water.

### Acknowledgements

This work was supported by the CSIR (Letter No. 01(2692)/12/EMR-II dated 03/10/2012) New Delhi. AS, SKT and ND are thankful to DST (Inspire programme), CSIR and UGC, New Delhi, India, respectively, for their fellowship. The authors sincerely acknowledge Dr. Mrinmoy De, Indian Institute of Science, Bangalore for his kind help in recorder TEM images of our samples. We are grateful to reviewers for their critical comments and valuable suggestion to improve the quality of the manuscript.

### Notes and references

School of Basic Sciences, Indian Institute of Technology Bhubaneswar, Bhubaneswar-751007, India. Tel: +91-674 2576053, E-mail: srikanta@iitbbs.ac.in,

†Electronic Supplementary Information (ESI) available: See <http://dx.doi.org/10.1039/b000000x/>

- D. Ferrer, A. Torres-Castro, X. Gao, S. Sepulveda-Guzman, U. Ortiz-Mendez and M. Jose-Yacamán, *Nano Lett.*, 2007, **7**, 1701-1705.
- J. D. Aiken III and R. G. Finke, *J. Mol. Catal. A: Chemical*, 1999, **145**, 1-44.
- S. Patra and H. Yang, *Bull. Kor. Chem. Soc.*, 2009, **30**, 1485-1488.
- Y. Kang, J. Snyder, M. Chi, D. Li, K. L. More, N. M. Markovic and V. R. Stamenkovic, *Nano Lett.*, 2014, **14**, 6361-6367.
- M. K. Debe, *Nature*, 2012, **486**, 43-51.
- Y. G. Sun and Y. N. Xia, *Science*, 2002, **298**, 2176-2179.
- V. Mazumder, M. Chi, K. L. More and S. Sun, *Angew. Chem. Int. Ed.*, 2010, **49**, 9368-9372.
- C. Wang, D. van der Vliet, K. L. More, N. J. Zaluzec, S. Peng, S. Sun, H. Daimon, G. Wang, J. Greeley, J. Pearson, A. P. Paulikas, G. Karapetrov, D. Strmcnik, N. M. Markovic and V. R. Stamenkovic, *Nano Lett.*, 2011, **11**, 919-926.
- M. B. Cortie and A. M. McDonagh, *Chem. Rev.*, 2011, **111**, 3713-3735.
- M. Rycenga, C. M. Cobley, J. Zeng, W. Y. Li, C. H. Moran, Q. Zhang, D. Qin and Y. N. Xia, *Chem. Rev.*, 2011, **111**, 3669-3712.
- K. Saha, S. S. Agasti, C. Kim, X. N. Li and V. M. Rotello, *Chem. Rev.*, 2012, **112**, 2739-2779.
- X. Zhang, S. Ye, X. Zhang and L. Wu, *J. Mater. Chem. C*, 2015, **3**, 2282-2290.
- N. Toshima and T. Yonezawa, *New J. Chem.*, 1998, **22**, 1179-1201.
- H. J. You, F. L. Zhang, Z. Liu and J. X. Fang, *ACS Catal.*, 2014, **4**, 2829-2835.
- H. M. Song, D. H. Anjum, R. Sougrat, M. N. Hedhili and N. M. Khashab, *J. Mater. Chem.*, 2012, **22**, 25003-25010.
- J. Zeng, Q. Zhang, J. Y. Chen and Y. N. Xia, *Nano Lett.*, 2010, **10**, 30-35.
- Y. J. Xiang, X. C. Wu, D. F. Liu, X. Y. Jiang, W. G. Chu, Z. Y. Li, Y. Ma, W. Y. Zhou and S. S. Xie, *Nano Lett.*, 2006, **6**, 2290-2294.
- M. Sastry, A. Swami, S. Mandal and P. R. Selvakannan, *J. Mater. Chem.*, 2005, **15**, 3161-3174.
- L. Wang and Y. Yamauchi, *J. Am. Chem. Soc.*, 2010, **132**, 13636-13638.
- K. Qian and W. X. Huang, *Catal. Today*, 2011, **164**, 320-324.
- P. Qiao, S. Xu, D. Zhang, R. Li, S. Zou, J. Liu, W. Yi, J. Li and J. Fan, *Chem. Commun.*, 2014, **50**, 11713-11716.
- N. Kristian, Y. S. Yan and X. Wang, *Chem. Commun.*, 2008, 353-355.
- S. Panigrahi, S. Basu, S. Praharaj, S. Pande, S. Jana, A. Pal, S. K. Ghosh and T. Pal, *J. Phys. Chem. C*, 2007, **111**, 4596-4605.
- D. Zhao and B. Q. Xu, *Phys. Chem. Chem. Phys.*, 2006, **8**, 5106-5114.
- D. Zhao and B. Q. Xu, *Angew. Chem. Int. Ed.*, 2006, **45**, 4955-4959.
- H. P. Liang, Y. G. Guo, H. M. Zhang, J. S. Hu, L. J. Wan and C. L. Bai, *Chem. Commun.*, 2004, 1496-1497.
- H. P. Liang, H. M. Zhang, J. S. Hu, Y. G. Guo, L. J. Wan and C. L. Bai, *Angew. Chem. Int. Ed.*, 2004, **43**, 1540-1543.
- H. P. Liang, L. J. Wan, C. L. Bai and L. Jiang, *J. Phys. Chem. B*, 2005, **109**, 7795-7800.
- M. Pradhan, J. Chowdhury, S. Sarkar, A. K. Sinha and T. Pal, *The J. Phys. Chem. C*, 2012, **116**, 24301-24313.
- M. Wang, W. Zhang, J. Wang, D. Wexler, S. D. Poynton, R. C. T. Slade, H. Liu, B. Winther-Jensen, R. Kerr, D. Shi and J. Chen, *ACS Appl. Mater. Interfaces*, 2013, **5**, 12708-12715.
- J. W. Hong, S. W. Kang, B. S. Choi, D. Kim, S. B. Lee and S. W. Han, *ACS Nano*, 2012, **6**, 2410-2419.
- C. Buchner, L. Lichtenstein, S. Stucklenholz, M. Heyde, F. Ringleb, M. Sterrer, W. E. Kaden, L. Giordano, G. Pacchioni and H. J. Freund, *J. Phys. Chem. C*, 2014, **118**, 20959-20969.
- X. Zhang, F. Zhang and K.-Y. Chan, *Catal. Commun.*, 2004, **5**, 749-753.
- S. W. Kang, Y. W. Lee, Y. Park, B.-S. Choi, J. W. Hong, K.-H. Park and S. W. Han, *ACS Nano*, 2013, **7**, 7945-7955.
- S. Khanal, N. Bhattarai, D. McMaster, D. Bahena, J. J. Velazquez-Salazar and M. Jose-Yacamán, *Phys. Chem. Chem. Phys.*, 2014, **16**, 16278-16283.
- L. Wang and Y. Yamauchi, *Chem. Mater.*, 2011, **23**, 2457-2465.
- W. Xu, H. Yi, Y. Yuan, P. Jing, Y. Chai, R. Yuan and G. S. Wilson, *Biosens. Bioelectron.*, 2015, **64**, 423-428.
- J.-W. Hong, Y.-W. Lee, M.-J. Kim, S.-W. Kang and S.-W. Han, *Chem. Commun.*, 2011, **47**, 2553-2555.
- C. Hsu, C. Huang, Y. Hao and F. Liu, *Electrochem. Commun.*, 2012, **23**, 133-136.
- H. M. Song, B. A. Moosa and N. M. Khashab, *J. Mater. Chem.*, 2012, **22**, 15953-15959.
- A. Renjith and V. Lakshminarayanan, *J. Mater. Chem. A*, 2015, **3**, 3019-3028.
- S. Nath, S. Praharaj, S. Panigrahi, S. K. Ghosh, S. Kundu, S. Basu and T. Pal, *Langmuir*, 2005, **21**, 10405-10408.
- P. S. S. Kumar, A. Manivel, S. Anandan, M. Zhou, F. Grieser and M. Ashokkumar, *Colloids Surf., A*, 2010, **356**, 140-144.
- Q. He, B. Shyam, M. Nishijima, X. Yang, B. Koel, F. Ernst, D. Ramaker and S. Mukerjee, *J. Phys. Chem. C*, 2013, **117**, 1457-1467.
- D. H. Lee, J. A. Lee, W. J. Lee, D. S. Choi, W. J. Lee and S. O. Kim, *J. Phys. Chem. C*, 2010, **114**, 21184-21189.
- H. Li, J. K. Jo, L. D. Zhang, C.-S. Ha, H. Suh and I. Kim, *Langmuir*, 2010, **26**, 18442-18453.
- J. Yang, J. Y. Lee and H.-P. Too, *Plasmonics*, 2006, **1**, 67-78.
- A. Shah, R. Latif ur, R. Qureshi and R. Ziaur, *Rev. Adv. Mater. Sci.*, 2012, **30**, 133-149.
- S.-R. Yuan, R. Yuan, Y.-Q. Chai, L. Mao, X. Yang, Y.-L. Yuan and H. Niu, *Talanta*, 2010, **82**, 1468-1471.
- R. Awasthi and R. N. Singh, *Carbon*, 2013, **51**, 282-289.
- K. M. K. Yu, P. Meric and S. C. Tsang, *Catal. Today*, 2006, **114**, 428-433.
- A. N. Grace and K. Pandian, *Electrochem. Commun.*, 2006, **8**, 1340-1348.
- P. Zhao, X. Feng, D. Huang, G. Yang and D. Astruc, *Coord. Chem. Rev.*, 2015, **287**, 114-136.
- A. Gangila, R. Podila, R. M. L. Karanam, C. Janardhana and A. M. Rao, *Langmuir*, 2011, **27**, 15268-15274.
- P. Zhao, L. Xinchun, G. Yang, D. Huang, X. Feng and Q. Xu, *New J. Chem.*, 2015, DOI: 10.1039/C5NJ00673B, Ahead of Print.
- N. Pradhan, A. Pal and T. Pal, *Colloids Surf. a-Physicochem. Eng. Aspects*, 2002, **196**, 247-257.
- S. Patra, J. Das and H. Yang, *Electrochim. Acta*, 2009, **54**, 3441-3445.
- M. A. Aziz, S. Patra and H. Yang, *Chem. Commun.*, 2008, 4607-4609.
- L. Ding, W. Li, Q. Sun, Y. He and B. Su, *Chem. Eur. J.*, 2014, **20**, 12777-12780.

60. B. Ballarin, M. C. Cassani, E. Scavetta and D. Tonelli, *Electrochim. Acta*, 2008, **53**, 8034-8044.
61. J. Du, Y. Wang, X. Zhou, Z. Xue, X. Liu, K. Sun and X. Lu, *J. Phys. Chem. C*, 2010, **114**, 14786-14793.
62. P. Kannan, S. Sampath and S. A. John, *J. Phys. Chem. C*, 2010, **114**, 21114-21122.
63. N. Atar, T. Eren, M. L. Yola, H. Karimi-Maleh and B. Demirdogen, *RSC Adv.*, 2015, **5**, 26402-26409.
64. Z. Aksu, *Process Biochem.*, 2005, **40**, 997-1026.
65. A. D. Bokare, R. C. Chikate, C. V. Rode and K. M. Paknikar, *Appl. Catal., B*, 2008, **79**, 270-278.
66. H. Gopalappa, K. Yogendra, K. M. Mahadevan and N. Madhusudhana, *Chem. Sci. Trans.*, 2014, **3**, 232-239, 238 pp.
67. Y.-h. Shih and C.-h. Lin, *Environ Sci Pollut Res Int*, 2012, **19**, 1652-1658.
68. A. Johnson, G. Merilis, J. Hastings, M. E. Palmer, J. P. Fitts and D. Chidambaram, *J. Electrochem. Soc.*, 2013, **160**, G27-G31.
69. X. Liu, W. Li, N. Chen, X. Xing, C. Dong and Y. Wang, *RSC Adv.*, 2015, **5**, 34456-34465.
70. A. Khanna and V. K. Shetty, *Sol. Energy*, 2014, **99**, 67-76.
71. C. Burda, US20060210798A1, 2006.
72. V. Subramanian, P. V. Kamat and E. E. Wolf, *Ind. Eng. Chem. Res.*, 2003, **42**, 2131-2138.
73. S. M. Ghoreishi and R. Haghghi, *Chem. Eng. J.*, 2003, **95**, 163-169.
74. S. X. Wu, Q. Y. He, C. M. Zhou, X. Y. Qi, X. Huang, Z. Y. Yin, Y. H. Yang and H. Zhang, *Nanoscale*, 2012, **4**, 2478-2483.
75. S. Nam and P. G. Tratnyek, *Water Research*, 2000, **34**, 1837-1845.
76. G. G. Glenner, *New Eng. J. Med.*, 1980, **302**, 1283-1292.
77. S. Caspi, M. Halimi, A. Yanai, S. B. Sasson, A. Taraboulos and R. Gabizon, *J. Biol. Chem.*, 1998, **273**, 3484-3489.
78. R. Pirola, E. Mundo, L. Bellodi and S. R. Bareggi, *J. Chromatogr. B*, 2002, **772**, 205-210.
79. M. Isik and D. T. Sponza, *J. Environ. Sci. Health A Tox. Hazard Subst. Environ. Eng.*, 2004, **39**, 1107-1127.
80. P. E. Diniz, A. T. Lopes, A. R. Lino and M. L. Serralheiro, *Appl. Biochem. Biotechnol.*, 2002, **97**, 147-163.
81. K. T. Chung, S. E. Stevens, Jr. and C. E. Cerniglia, *Crit. Rev. Microbiol.*, 1992, **18**, 175-190.
82. L. L. Barton and G. D. Fauque, in *Advanced Applied Microbiology*, eds. S. S. Allen I. Laskin and M. G. Geoffrey, Academic Press, 2009, vol. Volume 68, pp. 41-98.
83. C. C. Hsueh and B. Y. Chen, *J. Hazard Mater.*, 2007, **141**, 842-849.
84. S. Wada, H. Ichikawa and K. Tastsumi, *Biotechnol. Bioeng.*, 1995, **45**, 304-309.
85. Y. J. Kim and H. Uyama, *Cell. Mol. Life Sci.*, 2005, **62**, 1707-1723.
86. F. P. van der Zee and S. Villaverde, *Water Res.*, 2005, **39**, 1425-1440.
87. M. P. Shah, K. A. Patel, S. S. Nair and A. M. Darji, *Am. J. Microbiol. Res.*, 2014, **2**, 16-23.
88. A. Srinivasan and T. Viraraghavan, *J. Env. Manage.*, 2010, **91**, 1915-1929.
89. C. I. Pearce, J. R. Lloyd and J. T. Guthrie, *Dyes and Pigments*, 2003, **58**, 179-196.
90. T. Stephenson, *Biotechnol. Lett.*, 1990, **12**, 843-846.
91. P. Steinle, G. Stucki, R. Stettler and K. W. Hanselmann, *Appl. Environ. Microbiol.*, 1998, **64**, 2566-2571.
92. H. Kohler and H. Jenzer, *Free Rad. Biol. Med.*, 1989, **6**, 323-339.
93. L. Panda, B. Das, D. S. Rao and B. K. Mishra, *J. Hazard Mater.*, 2011, **192**, 822-831.
94. P. R. Rout, P. Bhunia and R. R. Dash, *J. Tai. Inst. Chem. Eng.*, 2015, **46**, 98-108.
95. H. M. Pinheiro, E. Touraud and O. Thomas, *Dyes and Pigments*, 2004, **61**, 121-139.
96. X. Liu, M. Atwater, J. Wang and Q. Huo, *Colloids Surf. B: Biointerfaces*, 2007, **58**, 3-7.
97. S. Gupta, C. Giordano, M. Gradzielski and S. K. Mehta, *J. Coll. Interface Sci.*, 2013, **411**, 173-181.
98. N. Daneshvar, A. Oladegaragoze and N. Djafarzadeh, *J. Hazard Mater.*, 2006, **129**, 116-122.

Treatment of azo dye-based waste water using new trimetallic porous Au@Pd@RuNPs and solid waste dolochar is described

